

See discussions, stats, and author profiles for this publication at: <https://www.researchgate.net/publication/244189310>

A computational study of lithium methoxide mixed aggregates with alkyllithiums

ARTICLE *in* TETRAHEDRON · MAY 2008

Impact Factor: 2.64 · DOI: 10.1016/j.tet.2008.03.022

CITATIONS

15

READS

30

4 AUTHORS, INCLUDING:



Ohyun Kwon

Samsung Advanced Institute of Technology

66 PUBLICATIONS 1,926 CITATIONS

SEE PROFILE



A computational study of lithium methoxide mixed aggregates with alkyllithiums

Lawrence M. Pratt^{a,*}, Ohyun Kwon^b, Thanh Chi Ho^c, Ngan Van Nguyen^c

^a Department of Chemistry, Fisk University, 1000 17th Ave. N., Nashville, TN 37209, United States

^b Samsung Advanced Institute of Technology, PO Box, 111, Suwon 440-600, South Korea

^c University of Pedagogy, 280 An Duong Vuong, District 5, Ho Chi Minh City, Viet Nam

ARTICLE INFO

Article history:

Received 22 January 2008

Received in revised form 6 March 2008

Accepted 7 March 2008

Available online 12 March 2008

ABSTRACT

The formation of alkyllithium–lithium methoxide mixed aggregates was modeled with the B3LYP density functional method. In the gas phase there was little tendency to form mixed dimers or trimers. Mixed tetramer formation was more energetically favorable, particularly for *tert*-butyllithium. THF solvation favored the formation of methyllithium and ethyllithium mixed tetramers, but not those of *sec*-butyllithium and *tert*-butyllithium. The potential for resolution of chiral alkyllithiums by mixed aggregate formation with enantiomerically pure lithium alkoxides was examined.

© 2008 Elsevier Ltd. All rights reserved.

1. Introduction

Organolithium mixed aggregates are complexes between two different lithium compounds, whose properties may be quite different from those of either pure component. Formation and synthetic applications of these species are the subject of a recent review.¹ The focus of this work was the formation of mixed aggregates between alkyllithiums and lithium alkoxides. A dimeric and a dodecameric mixed aggregate between *n*-propyllithium and lithium *n*-propoxide were reported in hydrocarbon solution.^{2,3} Mixed tetramers and mixed hexamers of *tert*-butyllithium and lithium *tert*-butoxide have also been reported in hydrocarbon solvents.^{4,5} Related mixed tetramers of lithium acetylides with lithium alkoxides in THF, diethyl ether, and solvent mixtures have also been reported.^{6,7} A lithium alkoxide–phenyllithium mixed dimer has also been reported.⁸ However, a literature search failed to reveal any systematic study of alkyllithium–lithium alkoxide mixed aggregate formation in polar solvents.

This particular type of mixed aggregate is of interest for several reasons. First, alkyllithiums exposed to small amounts of air form lithium hydroxide, peroxides, and alkoxides from the oxygen and water vapor, which can form mixed aggregates with the remaining alkyllithium. This can result in increased reactivity of the alkyllithium.⁹ Secondly, chiral alcohols are often obtained inexpensively from natural products, and the corresponding lithium alkoxide mixed aggregates with alkyllithiums have resulted in asymmetric induction for addition reactions.^{10,11} Finally, it has long

been known that secondary acyclic alkyllithiums can undergo rapid racemization, particularly in polar solvents.¹² This suggests the possibility of resolution of the alkyllithium enantiomers by formation of stable mixed aggregates with chiral lithium alkoxides.

In this paper we examined the formation of alkyllithium–lithium methoxide mixed dimers, trimers, and tetramers in the gas phase to determine the effects of increasing steric bulk of the alkyllithium. This also serves as an approximation to the behavior of these compounds in hydrocarbon solvents. Next, the effect of THF solvation was examined. Addition of polar solvents usually, but not always, breaks up higher aggregates into lower aggregates and/or monomers. Finally, the possible use of these mixed aggregates to resolve chiral alkyllithiums was examined.

2. Computational methods

All calculations were performed using *Gaussian 98* or *Gaussian 03*.¹³ The gas phase and solution energies reported include gas phase internal energy, thermal corrections to the free energy at 200 and 298.15 K, and where applicable, solvation terms. The temperature of 200 K was chosen as it is typical of dry ice–acetone bath temperatures, which are nominally -78°C or 195 K, but are usually slightly higher.

The solvation free energy change of the gas phase organolithium molecule $(\text{RLi})_n$ due to microsolvation by m explicit ethereal solvent ligands E (in this case, THF) is calculated by considering the process

$$(\text{RLi})_n + mE \rightarrow (\text{RLi})_n \cdot mE \quad (1)$$

The microsolvation model assumes that the free energy change accompanying this reaction adequately represents the solvation free energy $\Delta G_{\text{solv}}^{\circ}$ of the solute $(\text{RLi})_n$ in the solvent E , so that

* Corresponding author. Tel.: +1 615 3298559.

E-mail address: lp Pratt@fisk.edu (L.M. Pratt).

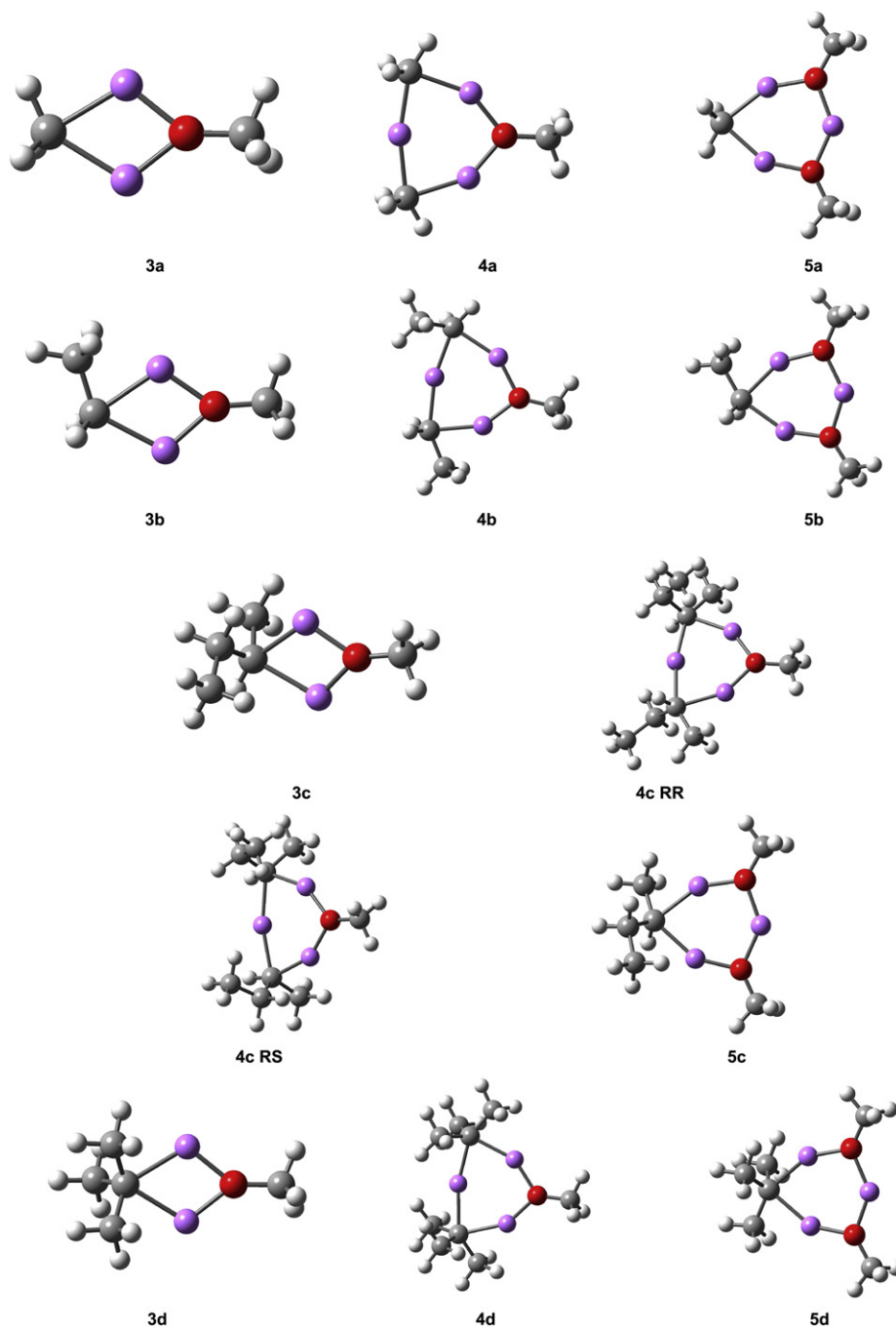


Figure 1. Optimized gas phase geometries of mixed dimers and mixed trimers. Gray: carbon; white: hydrogen; violet: lithium; red: oxygen.

Table 1

Calculated free energies of gas phase mixed dimer and mixed trimer formation (kcal/mol)

RLi/temp	(RLi)(LiOMe)		(RLi) ₂ (LiOMe)		(LiOMe) ₂ (RLi)	
	ΔG	ΔG per Li	ΔG	ΔG per Li	ΔG	ΔG per Li
MeLi/200	15.3	7.63	8.44	2.81	9.76	3.25
MeLi/298.15	12.3	6.13	6.22	2.07	7.32	2.44
EtLi/200	16.3	8.13	8.84	2.95	9.81	3.27
EtLi/298.15	13.6	6.82	6.68	2.22	7.36	2.45
<i>s</i> -BuLi/200	14.0	6.99	RR 6.56	RR 2.19	7.92	2.64
<i>s</i> -BuLi/298.15	11.4	5.71	4.39	1.46	5.60	1.87
<i>s</i> -BuLi/200			RS 4.91	RS 1.63		
<i>s</i> -BuLi/298.15			2.40	0.802		
<i>t</i> -BuLi/200	12.6	6.28	3.03	1.01	7.08	2.36
<i>t</i> -BuLi/298.15	9.51	4.76	0.454	0.151	4.69	1.56

$$G_T^{\circ}(\text{solute}) = G_T^{\circ}(\text{gas}) + \Delta G_{\text{solv}}^{\circ} \quad (2)$$

In other words, the free energy of a 'supermolecule' $(\text{RLi})_n \cdot m\text{E}$ relative to that of m solvent molecules is assumed to yield the free energy of the solvated molecule $(\text{RLi})_n$ in the condensed phase. The gas phase free energies of the relevant species are obtained computationally as

$$G_T^{\circ}(\text{gas}) = E_{\text{en}} + \Delta G_T^{\circ} \quad (3)$$

where the terms on the right hand side as well as the procedure used for calculating them are described below. The geometry of each molecule was first optimized using the B3LYP hybrid density functional method^{14,15} with the 6-31+G(d) basis set, followed by a calculation of vibrational frequencies at the same level of theory. Thus we have:

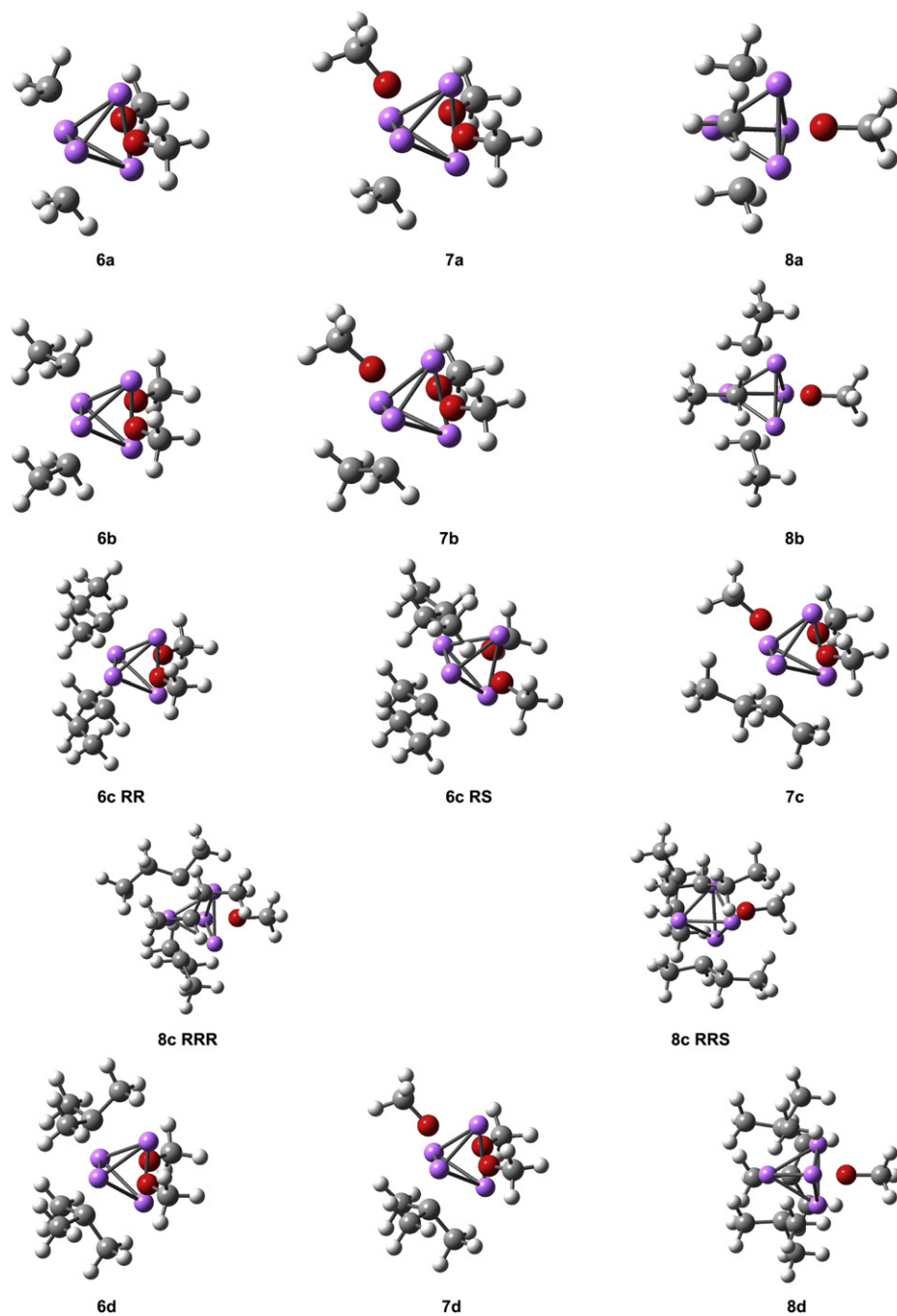


Figure 2. Optimized gas phase geometries of mixed tetramers.

Table 2

Calculated free energies of gas phase mixed tetramer formation (kcal/mol)

RLi/temp	(RLi) ₂ (LiOMe) ₂		(RLi)(LiOMe) ₃		(LiOMe)(RLi) ₃	
	ΔG	ΔG per Li	ΔG	ΔG per Li	ΔG	ΔG per Li
MeLi/200	−0.683	−0.171	−0.689	−0.172	−0.451	−0.113
MeLi/298.15	−0.707	−0.177	−0.770	−0.192	−0.458	−0.115
EtLi/200	−0.122	−0.0304	−0.544	−0.136	0.306	0.0766
EtLi/298.15	0.096	0.0240	−0.484	−0.121	0.741	0.185
<i>s</i> -BuLi/200	RR −1.07	RR −0.267	−1.56	−0.391	RRR −0.761	RRR −0.190
<i>s</i> -BuLi/298.15	−0.948	−0.237	−1.45	−0.363	−0.614	−0.154
<i>s</i> -BuLi/200	RS −0.96	RS −0.241			RRS −0.776	RRS −0.194
<i>s</i> -BuLi/298.15	−0.914	−0.228			−0.627	−0.157
<i>t</i> -BuLi/200	−5.91	−1.48	−4.45	−1.11	−4.95	−1.24
<i>t</i> -BuLi/298.15	−5.97	−1.49	−4.64	−1.16	−5.36	−1.34

Table 3

Calculated free energies of mixed dimer tetrasolvate formation from the disolvate (kcal/mol)

Mixed dimer	200 K	298.15 K
LiOMe–MeLi	0.80	5.18
LiOMe–EtLi	2.57	7.27
LiOMe– <i>s</i> -BuLi	2.92	7.73
LiOMe– <i>t</i> -BuLi	3.24	7.97

E_{en} = the electronic energy plus nuclear repulsion of the equilibrium geometry, using B3LYP/6-31+G(d),

E_0^{vib} = unscaled B3LYP vibrational zero point energy,

ΔG_T° = B3LYP thermal corrections to the free energy for a standard state of 1 atm and specified temperature from the masses. This includes contributions from translational, rotational, and vibrational degrees of freedom.

Calculations for the free energy changes for the 'reactions' (dimerizations, tetramerizations, mixed aggregate formation, etc.) are straightforward using the $G_T^\circ(\text{gas})$ terms defined in Eq. 2.

Correction terms are needed to convert the gas phase free energies to standard state of a solution, which is taken as 1 mol L^{−1}. The details of these corrections have been previously published.¹⁶ Briefly, a correction is required to convert the standard state of an ideal gas (1 atm) to the standard state of the solution. These corrections amount to 1.1120 kcal/mol at 200 K and 1.8943 kcal/mol at 298.15 K. These correction terms were included in all solution phase reactions below, i.e., calculations where the microsolvation model was used. Yet another correction is required for proper treatment of the explicit solvent molecules used in microsolvation. The traditional approach is to set the standard state of a pure liquid to be the concentration of the pure liquid itself, which then allows one to drop the concentration of the pure liquid from equilibria expressions (consider the ionic product of water, for example). However, since we have decided to adopt the standard state of 1 mol L^{−1} for all species, the free energy change for the process



is given by¹⁷

$$\Delta G^\circ = -RT \ln \frac{[(\text{RLi} \cdot \text{THF})_2]}{[\text{RLi} \cdot 2\text{THF}]^2} - 2RT \ln [\text{THF}] \quad (5)$$

The molarity of the THF solvent was calculated to be 13.26 at 200 K, and 12.33 at 298.15 K, from its tabulated density.¹⁸ The corrections due to the second term in the equation above amount to −1.0273 and −1.4883 kcal/mol per THF at 200 and 298.15 K, respectively. These corrections were included whenever free THF appeared on one side of the equation. However, for the mixed aggregate formation reactions in this paper, equal numbers of co-ordinated THF molecules appeared on each side of the equations, causing these terms to cancel.

Table 4

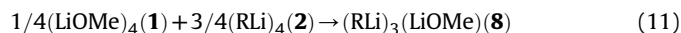
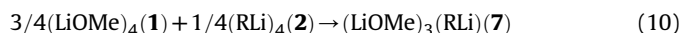
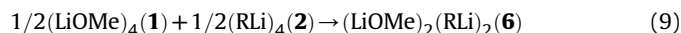
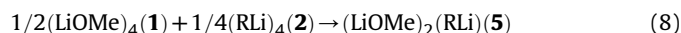
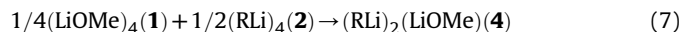
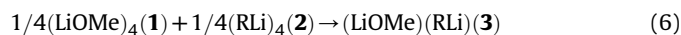
Calculated free energies of THF solvated mixed dimer and mixed trimer formation (kcal/mol)

RLi/temp	(RLi)(LiOMe)·2THF		(RLi) ₂ (LiOMe)·3THF		(LiOMe) ₂ (RLi)·3THF	
	ΔG	ΔG per Li	ΔG	ΔG per Li	ΔG	ΔG per Li
MeLi/200	6.25	3.12	3.82	1.27	7.32	2.44
MeLi/298.15	5.92	2.96	4.70	1.56	7.65	2.55
EtLi/200	5.22	2.61	4.92	1.64	8.71	2.90
EtLi/298.15	4.65	2.32	6.36	2.12	9.20	3.06
<i>s</i> -BuLi/200	4.98	2.49	RR 2.29	RR 0.763	7.00	2.33
<i>s</i> -BuLi/298.15	4.20	2.10	3.23	1.08	7.01	2.34
<i>s</i> -BuLi/200			RS 1.61	RS 0.536		
<i>s</i> -BuLi/298.15			2.55	0.849		
<i>t</i> -BuLi/200	6.04	3.02	9.23	3.08	7.81	2.60
<i>t</i> -BuLi/298.15	5.74	2.87	11.1	3.71	8.20	2.73

3. Results and discussion

3.1. Gas phase studies

Alkylolithiums typically exist as tetramers and higher aggregates in hydrocarbon solvents. The presence of several aggregates in equilibrium indicates that the free energy difference between them is small. Therefore, the alkylolithium and lithium methoxide tetramers were used as the basis for calculation of the free energies of mixed dimer, trimer, and tetramer formation in the gas phase.



2-8a R = CH₃; **2-8b** R = C₂H₅; **2-8c** R = *s*-Bu;

2-8d R = *t*-Bu

Since the *sec*-butyllithium exists as a set of fluxional aggregates (dimers, tetramers, and hexamers) in cyclopentane,¹⁹ the most stable *RRRR* diastereomer of the tetramer was used as the reference point. The energies of each diastereomeric aggregate containing two or more *sec*-butyllithium units were calculated separately.

The optimized geometries of the gas phase mixed dimers (**3**) and mixed trimers (**4** and **5**) are shown in Figure 1. Each of those species optimized to a structure containing a nearly planar ring containing the lithium, oxygen, and carbon atoms. The calculated free energies of mixed dimer and trimer formation are given in Table 1. Formation of these mixed aggregates was not particularly favorable compared to the homo-tetramers.

Figure 2 shows the optimized gas phase geometries of the mixed tetramers **6–8**, and the corresponding free energies of mixed tetramer formation are given in Table 2. Each mixed tetramer optimized to a tetrahedral structure. Compared to mixed dimer and mixed trimer formation, the mixed tetramer formation was energetically favorable. The free energies in Table 2 are consistent with

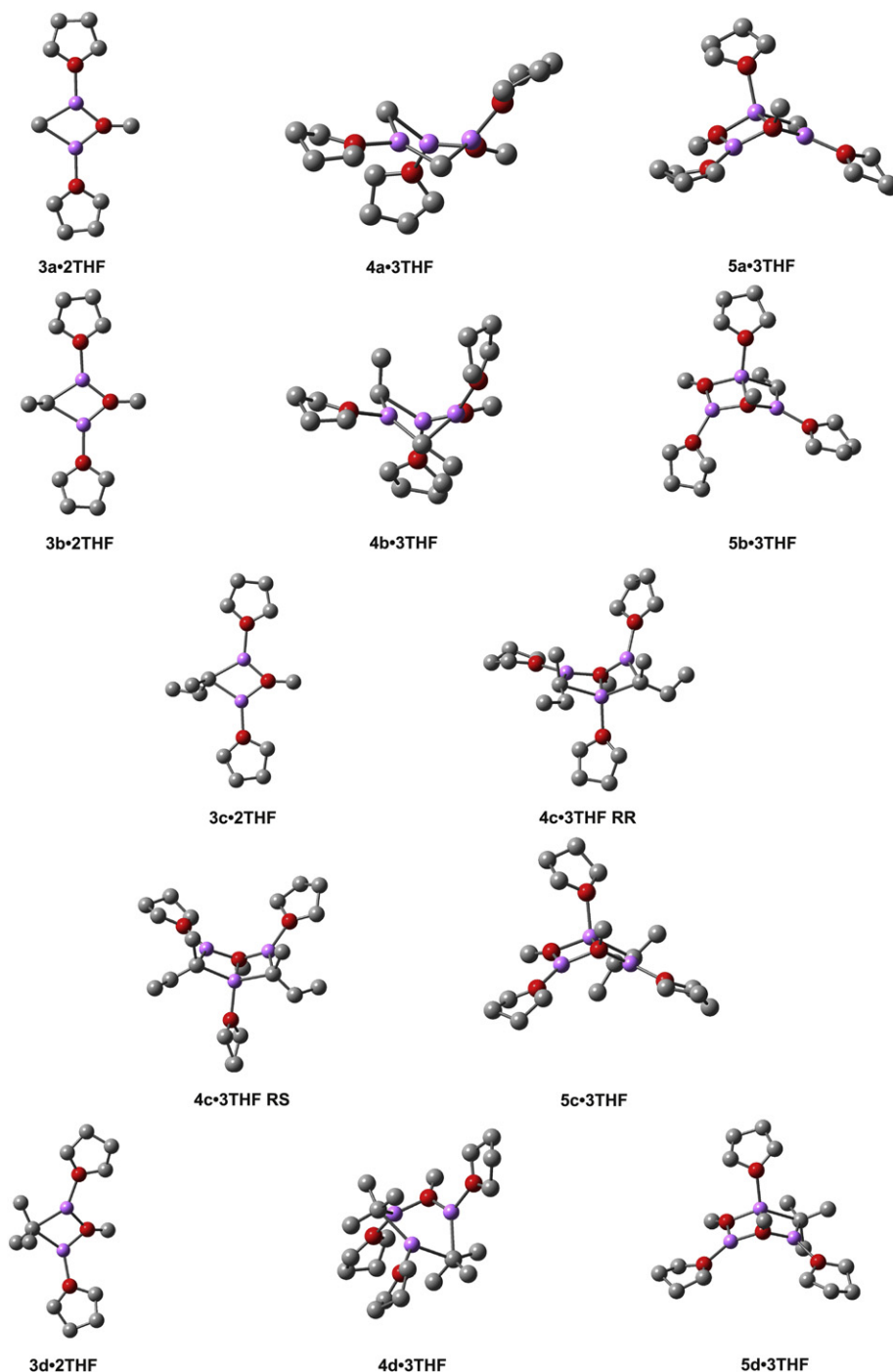


Figure 3. Optimized geometries of THF solvated mixed dimers and mixed trimers. Hydrogens omitted for clarity.

Table 5

Calculated free energies of THF solvated mixed tetramer formation (kcal/mol)

RLi/temp	(RLi) ₂ (LiOMe) ₂ ·4THF		(RLi)(LiOMe) ₃ ·4THF		(LiOMe)(RLi) ₃ ·4THF	
	ΔG	ΔG per Li	ΔG	ΔG per Li	ΔG	ΔG per Li
MeLi/200	−5.87	−1.47	−3.41	−0.853	−10.2	−2.54
MeLi/298.15	−3.31	−0.828	−2.07	−0.519	−7.27	−1.82
EtLi/200	−4.17	−1.04	−2.00	−0.500	−4.64	−1.16
EtLi/298.15	−1.50	−0.375	−0.263	−0.0657	−0.707	−0.177
s-BuLi/200	RR 1.18	RR 0.294	1.65	0.411	RRR 6.52	RRR 1.63
s-BuLi/298.15	4.46	1.11	3.91	0.977	11.3	2.84
s-BuLi/200	RS 1.54	RS 0.386			RRS 6.20	RRS 1.55
s-BuLi/298.15	4.83	1.21			10.7	2.69
t-BuLi/200	7.82	1.95	1.54	0.384	21.5	5.39
t-BuLi/298.15	12.5	3.12	4.00	0.999	27.7	6.91

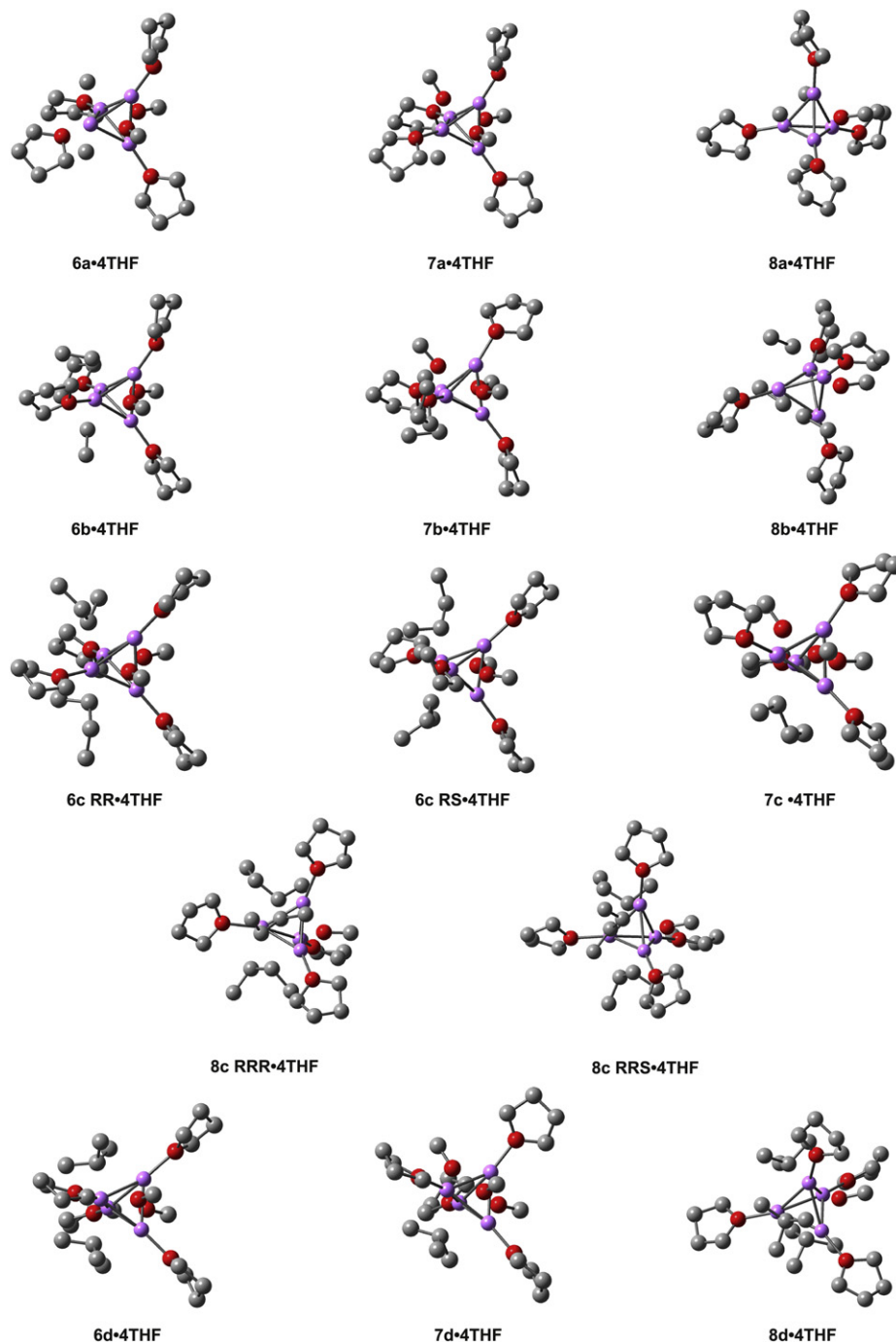


Figure 4. Optimized geometries of THF solvated mixed tetramers. Hydrogens omitted for clarity.

the tendency of *tert*-butyllithium to form mixed tetramers, and for less hindered alkylolithiums to form higher mixed aggregates in hydrocarbon solvents. The energies of mixed tetramer formation of *sec*-butyllithium showed little difference between the *RR* and *RS* diastereomers of $(s\text{-BuLi})_2(\text{LiOMe})_2$ or between the *RRR* and *RRS* diastereomers of $(\text{LiOMe})(s\text{-BuLi})_3$.

3.2. Studies in THF solution

Methyllithium has been found to be tetrameric in a 0.6 M solution in THF at 193 K.²⁰ In THF at 165–209 K, measurements reported by Bauer et al.²¹ show that *n*-butyllithium is a dimer–tetramer equilibrium, *sec*-butyllithium is a monomer–dimer equilibrium, and *tert*-butyllithium is a monomer; typical concentrations

for these measurements are 1.2–1.4 M. Three lithium NMR signals have been observed for ethyllithium in a 1:1 mixed solvent of THF and pentane at 158 K,²² which were tentatively assigned as the dimer, tetramer, and a small amount of hexamer. Since for most alkylolithiums the dimers are in equilibrium with other aggregates, the energy differences between these aggregates are small. Therefore, the dimers were used as the reference point for calculation of the free energies of mixed aggregate formation.

The aggregation state for THF solvated lithium methoxide was determined by calculating the free energy of the tetramer from the dimer.

$$2(\text{LiOMe})_2 \cdot 2\text{THF} \rightarrow (\text{LiOMe})_4 \cdot 4\text{THF} \quad (12)$$

Formation of the tetramer was exergonic by 24.0 and 20.7 kcal/mol at 200 and 298.15 K, respectively. The lithium methoxide tetrasolvated

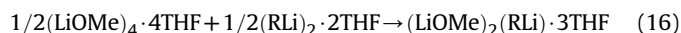
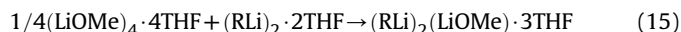
tetramer was therefore used in the subsequent calculations for the free energies of mixed aggregate formation.

Homo- or mixed dimers can potentially exist in THF solution with either one or two THF ligands per lithium atom. We have previously shown that the solvation state of alkyllithium dimers varies with temperature and steric bulk, and that the disolvated dimer is favored at higher temperatures and with *sec*- and *tert*-butyllithium.²³ The disolvated alkyllithium dimers were used as the reference state in this paper. The free energies of mixed dimer tetrasolvates were calculated from the disolvated by



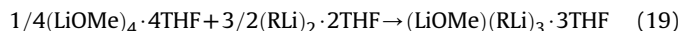
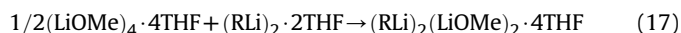
The free energies of tetrasolvate formation are shown in Table 3, and include corrections for the standard state of free THF, as described in Section 2. These energies were endergonic by 0.8–3.2 kcal/mol at 200 K and by 5.2–8.0 kcal/mol at 298.15 K. Therefore, the disolvated (one THF per lithium atom) mixed dimers were used in subsequent calculations. Since higher mixed aggregates are even more sterically hindered, their free energies of formation in THF solution were calculated using one THF ligand per lithium atom.

The free energies of THF solvated mixed dimers and mixed trimers were calculated according to Eqs. 14–16, and the results are shown in Table 4. Figure 3 shows the optimized geometries. In contrast to the planar mixed trimers in the gas phase, the THF solvated mixed trimers adopted boat-like or ladder-like conformations of the lithium–oxygen–carbon backbone. As in the gas phase, mixed dimer and mixed trimer formation was not particularly favorable, although solvation favored the mixed dimer formation by about 3–6 kcal/mol over the gas phase, and the $(\text{RLi})_2(\text{LiOMe})$ mixed trimer by about 1–2 kcal/mol. The free energies of formation for the solvated $(\text{LiOMe})_2(\text{RLi})$ mixed trimers were similar to those in the gas phase.



The free energies of THF solvated mixed tetramer formation were calculated according to Eqs. 17–19, and the energies are reported in

Table 5. The optimized geometries are shown in Figure 4. THF solvation favors the formation of methyllithium and ethyllithium mixed tetramers, but apparently disfavors the formation of the *sec*-butyllithium and *tert*-butyllithium mixed tetramers because of increased steric effects. This does not necessarily mean that the mixed tetramers do not form in THF solution, but if they are formed, the tetramer units may not be strongly coordinated to four THF ligands, and bulk solvent effects may be dominant in those systems. It was instructive to examine the formation of mixed tetramers of (*R*)-lithium *sec*-butoxide with *R* and *S* *sec*-butyllithium, as described below.



The preceding calculations indicate that the tetramer is the most stable mixed aggregate relative to the mixed dimer and trimers, and that in the absence of coordinating solvent molecules, the $(\text{RLi})_2(\text{LiOMe})_2$ mixed tetramer is usually favored. It is therefore instructive to examine similar mixed tetramers with chiral lithium alkoxides to estimate how effective they might be in resolving racemic *sec*-butyllithium. For this purpose, we examined the formation of the mixed tetramers of lithium (*R*)-2-butoxide and the lithium alkoxide of (1*R*,2*S*,5*R*)-menthol. The mixed tetramers were modeled with two monomer units of *sec*-butyllithium in the *RR*, *RS*, and *SS* configurations. The energy of each mixed tetramer was calculated relative to the most stable form, which is the *RR* diastereomer with lithium (*R*)-2-butoxide and the *SS* diastereomer with the lithium alkoxide of menthol. The optimized geometries are shown in Figure 5, and the energies are given in Table 6.

The next most stable diastereomer of the lithium (*R*)-2-butoxide mixed tetramer is the *RS* configuration. The free energy difference is 0.474 and 0.577 kcal/mol at 200 and 298.15 K, respectively. This corresponds to equilibrium constants for the interconversion of 0.30 and 0.38 at the respective temperatures. The lithium alkoxide of menthol is predicted to be somewhat better for the resolution of racemic *sec*-butyllithium, with free energy differences between the *SS* and the next most stable *RS* diastereomers of 0.909 and

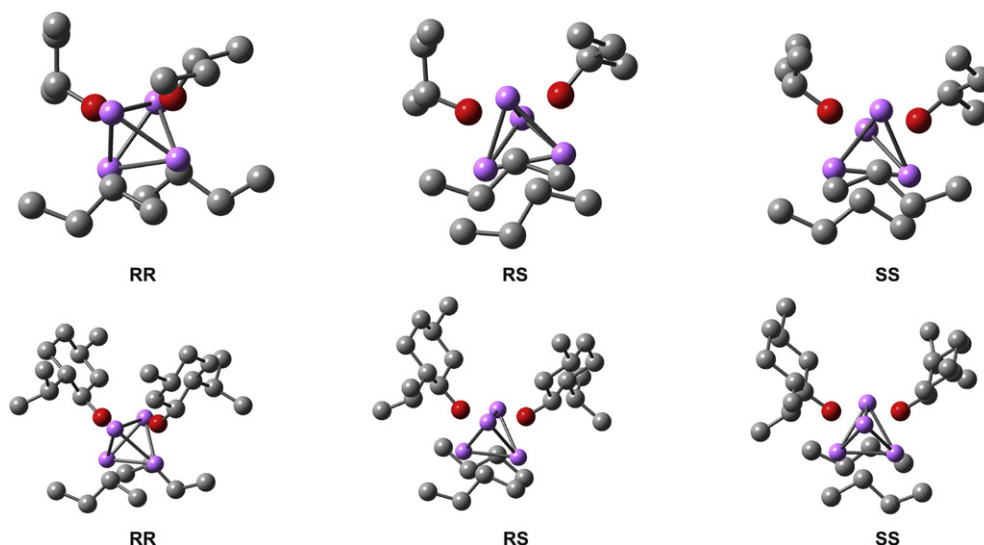


Figure 5. Optimized geometries of $(\text{RLi})_2(\text{LiOMe})_2$ mixed tetramers of *sec*-butyllithium with chiral lithium alkoxides. Top row: lithium (*R*) *sec*-butoxide; bottom row: lithium alkoxide of menthol.

Table 6

Relative free energies of *sec*-butyllithium mixed tetramers with chiral lithium alkoxides (kcal/mol)

R–OLi	Temp (K)	RR	RS	SS
(<i>R</i>) <i>s</i> -BuOLi	200	0	0.474	0.604
(<i>R</i>) <i>s</i> -BuOLi	298.15	0	0.577	0.794
Menthol	200	1.18	0.909	0
Menthol	298.15	1.40	0.993	0

0.993 kcal/mol, respectively, at 200 and 298.15 K. The corresponding equilibrium constants are 0.09 and 0.19 for the interconversion of the two diastereomers. Since these structures are rather sterically hindered, the gas phase structures will likely provide good approximations for the energy differences in weakly coordinating solvents. Even THF may not strongly bind to each lithium atom because of steric effects. Changing the solvent will likely have some influence on the resolution of racemic alkyllithiums, as will the chiral lithium alkoxide structure.

4. Conclusions

Alkyllithiums form mixed aggregates with lithium methoxide, with mixed tetramers or higher aggregates being favored over mixed dimers and trimers. Mixed tetramers of methyllithium and ethyllithium are solvated by one THF ligand per lithium atom, but steric effects may reduce the coordination of solvent ligands in more hindered aggregates. Comparison of the free energies of formation of diastereomeric mixed tetramers of chiral lithium alkoxides shows the potential of these species for resolution of racemic alkyllithiums.

Acknowledgements

This research used resources of the National Energy Research Scientific Computing Center, which is supported by the Office of Science of the U.S. Department of Energy under Contract No. DE-AC03-76SF00098. This work was also supported by NSF grant #INT-0454045.

Supplementary data

Tables of optimized geometries and energies of all aggregates are provided. Supplementary data associated with this article can be found in the online version, at doi:10.1016/j.tet.2008.03.022.

References and notes

- Pratt, L. M. *Mini-Rev. Org. Chem.* **2004**, *1*, 209.
- Thomas, R. D.; Huang, H. J. *Am. Chem. Soc.* **1999**, *121*, 11239.
- DeLong, G. T.; Hoffmann, D.; Nguyen, H. D.; Thomas, R. D. *J. Am. Chem. Soc.* **1997**, *119*, 11998.
- Thomas, R. D.; Jensen, R. M.; Yound, T. C. *Organometallics* **1987**, *6*, 565.
- Bates, T. F.; Clarke, M. T.; Thomas, R. D. *J. Am. Chem. Soc.* **1988**, *110*, 5109.
- Briggs, T. F.; Winemiller, M. D.; Xiang, B.; Collum, D. B. *J. Org. Chem.* **2001**, *66*, 6291.
- Parsons, R. L., Jr.; Fortunak, J. M.; Dorow, R. L.; Harris, G. D.; Kauffman, G. S.; Nugent, W. A.; Winemiller, M. D.; Briggs, T. F.; Xiang, B.; Collum, D. B. *J. Am. Chem. Soc.* **2001**, *123*, 9135.
- Fressigne, C.; Lautrette, A.; Maddaluno, J. J. *Org. Chem.* **2005**, *70*, 7816.
- McGarrity, J. F.; Ogle, C. A.; Brich, Z.; Loosli, H.-R. *J. Am. Chem. Soc.* **1985**, *107*, 1810.
- Pierce, M. E.; Parsons, R. L.; Radesca, L. A.; Lo, Y. S.; Silverman, S.; Moore, J. R.; Islam, Q.; Choudhury, A.; Fortunak, J. M. D.; Nguyen, D.; Luo, C.; Morgan, S. J.; Davis, W. P.; Confalone, P. N.; Chen, C.; Tillyer, R. D.; Frey, L.; Tan, L.; Xu, F.; Zhao, D.; Thompson, A. S.; Corley, E. G.; Grabowski, E. J. J.; Reamer, R.; Reider, P. J. *J. Org. Chem.* **1998**, *63*, 8536.
- Kauffman, G. S.; Harris, G. D.; Dorow, R. L.; Stone, B. R. P.; Parsons, R. L., Jr.; Pesti, J. A.; Magnus, N. A.; Fortunak, J. M.; Confalone, P. N.; Nugent, W. A. *Org. Lett.* **2000**, *2*, 3119.
- Witanowski, M.; Roberts, J. D. *J. Am. Chem. Soc.* **1966**, *88*, 737.
- Frisch, M. J.; Trucks, G. W.; Schlegel, H. B.; Scuseria, G. E.; Robb, M. A.; Cheeseman, J. R.; Montgomery, J. A., Jr.; Vreven, T.; Kudin, K. N.; Burant, J. C.; Millam, J. M.; Iyengar, S. S.; Tomasi, J.; Barone, V.; Mennucci, B.; Cossi, M.; Scalmani, G.; Rega, N.; Petersson, G. A.; Nakatsuji, H.; Hada, M.; Ehara, M.; Toyota, K.; Fukuda, R.; Hasegawa, J.; Ishida, M.; Nakajima, T.; Honda, Y.; Kitao, O.; Nakai, H.; Klene, M.; Li, X.; Knox, J. E.; Hratchian, H. P.; Cross, J. B.; Adamo, C.; Jaramillo, J.; Gomperts, R.; Stratmann, R. E.; Yazyev, O.; Austin, A. J.; Cammi, R.; Pomelli, C.; Ochterski, J. W.; Ayala, P. Y.; Morokuma, K.; Voth, G. A.; Salvador, P.; Dannenberg, J. J.; Zakrzewski, V. G.; Dapprich, S.; Daniels, A. D.; Strain, M. C.; Farkas, O.; Malick, D. K.; Rabuck, A. D.; Raghavachari, K.; Foresman, J. B.; Ortiz, J. V.; Cui, Q.; Baboul, A. G.; Clifford, S.; Cioslowski, J.; Stefanov, B. B.; Liu, G.; Liashenko, A.; Piskortz, P.; Komaromi, I.; Martin, R. L.; Fox, D. J.; Keith, T.; Al-Laham, M. A.; Peng, C. Y.; Nanayakkara, A.; Challacombe, M.; Gill, P. M. W.; Johnson, B.; Chen, W.; Wong, M. W.; Gonzalez, C.; Pople, J. A. *Gaussian 03, Revision A.1*; Gaussian: Pittsburgh, PA, 2003.
- Becke, A. D. *J. Chem. Phys.* **1993**, *98*, 5648.
- Stephens, P. J.; Devlin, F. J.; Chabalowski, G. C.; Frisch, M. J. *J. Phys. Chem.* **1994**, *98*, 11623.
- Pratt, L. M.; Merry, S.; Nguyen, S. C.; Quan, P.; Thanh, B. T. *Tetrahedron* **2006**, *62*, 10821.
- Thompson, J. D.; Cramer, C. J.; Truhlar, D. G. *J. Chem. Phys.* **2003**, *119*, 1661.
- Govender, U. P.; Letcher, T. M.; Garg, S. K.; Ahluwalia, J. C. *J. Chem. Eng. Data* **1996**, *41*, 147.
- Fraenkel, G.; Henrichs, M.; Hewitt, M.; Su, B. M. *J. Am. Chem. Soc.* **1984**, *106*, 255.
- McKeever, L. D.; Waack, R.; Doran, M. A.; Baker, E. B. *J. Am. Chem. Soc.* **1969**, *91*, 1057.
- Bauer, W.; Winchester, W. R.; Schleyer, P. v. R. *Organometallics* **1987**, *6*, 2371.
- Pratt, L. M.; Newman, A.; St. Cyr, J.; Johnson, H.; Miles, B.; Lattier, A.; Austin, E.; Henderson, S.; Hershey, B.; Lin, M.; Balamraju, Y.; Sammonds, L.; Cheramie, J.; Karnes, J.; Hymel, E.; Woodford, B.; Carter, C. *J. Org. Chem.* **2003**, *68*, 6387.
- Pratt, L. M.; Truhlar, D. G.; Cramer, C. J.; Kass, S. R.; Thompson, J. D.; Xidos, J. D. *J. Org. Chem.* **2007**, *72*, 2962.